Article

Discovery Medicine 2023; 35(177): 483–491
https://doi.org/10.24976/Discov.Med.202335177.49

Low Dose of 5-Aminolevulinic Acid Hydrochloride Alleviates the Damage in Cardiomyocytes Induced by Lenvatinib via PI3K/AKT Signaling Pathway

Yun Shi[1,†], Fengying Hu[2,†], Hao Fu[3], Shaojie Li[3], Chengzhi Lu[2,4,*], Chunxiu Hu[3,*]

[1]The Fourth Central Clinical School, Tianjin Medical University, 300192 Tianjin, China
[2]The First Central Clinical School, Tianjin Medical University, 300142 Tianjin, China
[3]Department of Reproductive Medicine, Characteristic Medical Center of PAP, 300162 Tianjin, China
[4]Departmeng of Cardiology, Tianjin First Center Hospital, 300192 Tianjin, China
*Correspondence: lucz8@126.com (Chengzhi Lu); yuanmenghcx@163.com (Chunxiu Hu)
[†]These authors contributed equally.
Published: 1 August 2023

Background: Lenvatinib is an oral tyrosine kinase inhibitor (TKI), and has been applied in the clinical trials for the treatment of hepatocellular carcinoma (HCC). The function of 5-aminolevulinic acid hydrochloride (ALA) treatment in protecting cardiomyocytes under lenvatinib stimulation was investigated.
Methods: H9c2 cells were treated with 2 mg/mL lenvatinib for 48 h and 1 mM ALA in the lenvatinib with low dose 5-aminolevulinic acid treatment group (LL) group, 10 mM ALA in the lenvatinib with high-dose 5-aminolevulinic acid treatment group (LH) group and cells without treatment were used as an internal control. C57/BL mice were treated with 10 mg/kg lenvatinib and 200 mg/kg ALA in the LL group and 400 mg/kg ALA in the LH group by gavage once per day for 4 weeks. The proliferation ability of cells was detected using the methyl thiazolyl tetrazolium (MTT) assay. Target gene expression was calculated through real-time quantitative PCR (qPCR), and target protein expression was calculated through Western blotting analysis. The concentrations of cardiovascular protective factors were detected using enzyme linked immunosorbent assay (ELISA).
Results: In these experiments, 10 mM ALA significantly increased the viability rate of cardiomyocytes (105.4 $\pm$ 8.0%) compared with the single lenvatinib treatment group (73.2 $\pm$ 6.5%). We also noticed that activation of nuclear factor erythroid 2-related factor 2 (Nrf2)/heme oxygenase-1 (HO-1) and phosphatidylinositol-3-kinase (PI3K)/protein kinase B (AKT)/mammalian target of rapamycin (mTOR) pathways were activated after low-dose ALA treatment. 5-ALA treatment led to the downregulation of intercellular cell adhesion molecule-1 (ICAM-1) (0.81- and 0.71-fold), vascular cell adhesion molecule (VCAM) (0.63- and 0.66-fold), angiotensin I (ANGI) (0.88- and 0.66-fold), ANGII (0.66- and 0.48-fold) and upregulation of endothelial nitric oxide synthases (eNOS) (1.25- and 1.89-fold) compared with non 5-ALA treatment group.
Conclusions: With more experiments on animal models, low-dose of ALA treatment might be a therapeutic strategy to alleviate the damage to cardiomyocytes induced by lenvatinib.

Keywords: 5-aminolevulinic acid hydrochloride; lenvatinib; hepatocellular carcinoma; antitumor effect; cardiovascular; signaling pathway

Impact Statement

The present study showed that low-dose 5-aminolevulinic acid hydrochloride (5-ALA) treatment relieved the side effects of lenvatinib in the treatment of hepatocellular carcinoma (HCC) using *in vivo* and *in vitro* experiments. These factors might contribute to the clinical treatment of HCC patients, increase the survival rate of patients, and reduce the cost to public health.

Introduction

Hepatocellular carcinoma (HCC) is the fifth most common cancer and the third leading cause of cancer-related mortality. Although the overall prognosis of HCC has improved in the past decade, the survival time remains at a low level. According to a previous study, the 2-year survival time of HCC patients is less than 50%, and the 5-year survival time is only 10% in the USA [1]. Lenvatinib is an inhibitor of vascular endothelial growth factor (VEGF) receptors, fibroblast growth factor receptors (FGFRs) and platelet-derived growth factor receptors (PGFRs) [2]. These receptors all perform critical roles in angiogenesis, which is an important process in tumor growth and progression. Inhibition of these receptors decreased tumor size and inhibited cancer progression [3]. Lenvatinib is metabolized in the liver via the hepatic enzymes CYP3A4 (Cytochrome P450 3A4) and aldehyde ox-

idase. The half-life of lenvatinib is approximately 28 h, and the peak effect occurs 1 to 4 h after consumption [4]. However, lenvatinib treatment leads to the occurrence of hypertension in patients by inducing dysfunction in vascular cardiomyocytes [5–7]. 5-aminolevulinic acid hydrochloride (5-ALA) is a precursor of phototoxic protoporphyrin IX (PpIX), and the first step of heme synthesis is the formation of ALA from glycine and succinyl-coenzyme A [8]. Clinical trials have investigated the therapeutic effects of ALA on tumor cells, and ALA is a potential diagnostic and therapeutic agent [9–11]. A previous study showed that 5-ALA contributes to the treatment of cardiovascular disease due to its ability to promote the production of PpIX in HMEC-1 cells [12]. In addition, a previous study also indicated that 5-ALA might be superior in the accumulation of conventional sensitizers in endothelial cells [13]. Herein, we hypothesized that treatment with low concentration of ALA may exhibit a protective effect on cardiomyocytes and reduce the damage in cardiomyocytes induced by lenvatinib.

Materials and Methods

Material

H9c2 (GNR 5) cells were obtained from a typical culture cell bank of the Chinese Academy of Sciences (Shanghai, China). The cell line was tested for mycoplasma and STR (short tandem repeat) identification. H-DMEM (Dulbecco's Modified Eagle Medium) (10569010) and FBS (fetal bovine serum) (10100) were purchased from Gibco (NY, USA). FastDigest BsmBI (ER0451) and Lipo 3000 (L3000015) were purchased from Thermo (NY, USA). T4 PNK (T4 Polynucleotide Kinase) (M0201S) and Quick Ligase (M2200) were purchased from NEB (Beijing, China). Lenvatinib (E7080) was purchased from Selleck (NY, USA). 5-Aminolevulinic acid hydrochloride (ALA, A7793) was purchased from Sigma (MA, USA). p-AKT (protein kinase B) (ab38449), p-mTOR (mammalian target of rapamycin) (ab109268), p-ERK (extracellular regulated protein kinases) (ab214036), AKT (ab179463), mTOR (ab2732), ERK (ab17942), nuclear factor erythroid 2-related factor 2 (Nrf2) (ab137550), heme oxygenase-1 (HO-1) (ab13248), HIF-1α (hypoxia-inducible factor-1α) (ab179483), eNOS (endothelial nitric oxide synthases) (ab76198), VCAM-1 (vascular cell adhesion molecule-1) (ab134047), ICAM-1 (intercellular cell adhesion molecule-1) (ab2213), ACE (angiotensin-converting enzyme) I (ab75762), ACE II (ab87436), p-NF-κB (nuclear factor kappa-B) (ab222494), and NF-κB (ab207297) antibodies were purchased from Abcam (Cambridge, UK). The Nitric Oxide (NO) Assay Kit (A013-2-1), Angiotensin II (ANG II) Assay Kit (H185), and Vascular Endothelial Growth Factor-α (VEGF-α) Assay Kit (H044) were obtained from Nanjing Jiancheng Bioengineering Institute (Nanjing, China). The Reactive Oxygen Species (ROS) Assay Kit (S0033) was obtained from Beyotime (Beijing, China). Methyl thiazolyl tetrazolium (MTT) (M8180) and the Total RNA Extraction Kit (R1200) were purchased from Solarbio (Beijing, China). HiFiScript cDNA (complementary DNA) Synthesis Kit (CW2569) and SuperStar Probe One Step real-time quantitative PCR (RT-qPCR) Kit (CW2695) were purchased from CWbio (Beijing, China).

Animal Treatment

Twenty 10-week-old C57/BL mice were obtained from the Guangdong Medical Laboratory Animal Center. Mice were kept in a 37 °C atmosphere with a 12 h light/dark cycle with *ad libitum* access to water and food. Mice were divided into the control group (NC), lenvatinib treatment group (LT), lenvatinib with high-dose 5-aminolevulinic acid treatment group (LH), and lenvatinib with low-dose 5-aminolevulinic acid treatment group (LL). Mice were treated with 10 mg/kg lenvatinib [14], 200 mg/kg ALA in the LL group and 400 mg/kg ALA in the LH group for 4 weeks [15]. Heart tissue and serum samples were collected from the veins of mice after treatment to perform the following experiments. All mouse protocols were approved by Tianjin Medical University, and experiments were performed under institutional guidelines. Mice were anesthesia with isoflurane before model construction.

Cell Culture Method and MTT Assay

Cells were cultured in H-DMEM supplemented with 10% FBS at 37 °C in a humidified atmosphere with 5% CO_2. Cells were seeded in a 96-well plate at 1×10^5/well and cultured for 24 h prior to performing the MTT assay. Cells treated with 0.5, 1, 3, 5, or 10 mM ALA for 4 h or treated with 0.5, 1, 2, 5, or 10 mg/mL lenvatinib. Then, the cells were incubated with MTT reagent for 4 h. The OD (optical density) value at 490 nm was detected using a microplate reader (1410101, Thermo, Waltham, MA, USA). Cell viability was calculated as follows: viability rate = $(OD_{treatment} - OD_{Blank})/(OD_{Control} - OD_{Blank}) \times 100\%$. Cells cultured for other experiments were seeded in 100-mm dishes and divided into the control group (NC), lenvatinib treatment group (LT), lenvatinib with low dose 5-aminolevulinic acid treatment group (LL), and lenvatinib with high dose 5-aminolevulinic acid treatment group (LH).

RNA Extraction and Reverse Transcription

RNA extraction was performed in compliance with the manufacturer's protocol. Cells and heart tissues from mice were lysed with lysis buffer followed by incubation with chloroform. RNA in the water phase was collected in a collection tube after centrifugation for 10 min at 12,000 rpm. RNA was eluted with elution buffer after washing, and the concentration of RNA was measured using an Evolution 300 (Thermo, MA, USA). RNA template was added to the mixture of reaction buffer, as recommended in the protocol of the HiFiScript cDNA Synthesis Kit. The reaction was performed with the following steps: 42 °C for 15 min and

Table 1. Primers used for qPCR.

	Forward (5′-3′)	Reverse (5′-3′)
Nrf2	ACCGGAGAACCTCCCAAT	AGCTCCTGCCAAACTTGCTC
HO-1	AGCCCCACCAAGTTCAAACA	TGCCAACAGGAAGCTGAGAG
Fas	TCTGGATCCTTCCTCTTTGC	TCTGGATCCTTCCTCTTTGC
CDK6	GGTCAGGTTGTTTGATGTGTG	TCGGTGTGAATGAAGAAAGTCC
GAPDH	ACAGTCCATGCCATCACTG	AGTAGAGGCAGGGATGATG

85 °C for 5 min. Acquired cDNA was stored at –80 °C until subsequent experiments were performed.

Quantitative Polymerase Chain Reaction (qPCR)

The reaction mixture was composed according to the protocol, and the same amount of cDNA was used in each group. The following reaction protocol was used: 45 °C for 20 min; 95 °C for 5 min; and 40 cycles of 95 °C for 15 s and 60 °C for 35 s. The primers used for qPCR are listed in Table 1. Relative mRNA (messenger RNA) expression changes were calculated by $2^{-\Delta\Delta Cq}$ [16]. GAPDH (glyceraldehyde-3-phosphate dehydrogenase) was used as an internal control.

Western Blotting Analysis

Proteins from cell and tissue samples were lysed with lysis buffer (8 M urea, 50 mM IAA (Iodoacetamide), 10 mM DTT and a proteinase inhibitor cocktail) using ultrasonication. Samples were centrifuged, and supernatants were collected. Protein concentrations were determined using a BCA (Bicinchoninic Acid) assay. Then, the same amount of sample was used to perform electrophoresis. Separated proteins were transferred onto nitrocellulose membranes using the Trans-Blot Turbo transfer system (Bio-Rad, CA, USA). Membranes were initially incubated with 5% skim milk for 1 h at room temperature followed by overnight incubation with primary antibodies (p-AKT, p-mTOR, p-ERK, AKT, mTOR, ERK, Nrf2, HO-1, HIF-1α, eNOS, VCAM-1, ICAM-1, ACE I, ACE II, p-NF-κB, and NF-κB, dilution 1:1000) at 4 °C. The gray value of each band was detected using chemiluminescence after incubation with a secondary antibody (goat anti rabbit or mouse, dilution 1:5000) for 1 h at room temperature. The gray value of each band was analyzed and calculated using Image-Pro Plus (version 6.0, Rockville, MD, USA). GAPDH was used as an internal control.

ELISA

ELISA (enzyme linked immunosorbent assay) was performed according to the following protocol to detect the concentrations of NO, VEGF-α, ROS and ANG in cultured medium and serum samples from the mouse model. Briefly, cultured media and serum samples were mixed with reaction buffer and incubated at 37 °C for an appropriate reaction period. TMB (3,3',5,5'-Tetramethylbenzidine) substrate was added, and the OD value was detected at an appropriate wavelength.

Statistical Analysis

Data are presented as the mean ± SD. Each experiment was repeated three times independently. Differences between groups were calculated using one-way ANOVA (Analysis of Variance). $p < 0.05$ was considered as a significant difference ($^{*}p < 0.05$ compared to the NC group; and $^{\#}p < 0.05$ compared to the LT group).

Results

Effect of Lenvatinib and ALA Treatment on Cardiomyocytes.

Fig. 1 shows that the viability rates in each group under 0.5, 1, 3, 5, and 10 mM ALA treatment for 4 h were 110.3 ± 8.7, 135.4 ± 11.2, 115.1 ± 10.6, 103.2 ± 9.4, and 85.1 ± 7.1%, respectively. ALA treatment (1 mM) significantly increased the survival ability of cardiomyocytes ($p < 0.05$), while the high dose of ALA significantly decreased the survival ability ($p < 0.05$). The viability rates in each group under different concentrations of lenvatinib treatment were 89.2 ± 7.2, 84.1 ± 7.3, 69.1 ± 5.8, 56.2 ± 5.3 and 49.3 ± 4.1%. Lenvatinib treatment at 2, 5 and 10 mg/mL significantly decreased the viability rates of cardiomyocytes ($p < 0.05$). Therefore, we used 1 mM ALA treatment for 4 h and 2 mg/mL lenvatinib treatment in subsequent experiments. We next detected the viability rate in each group of cardiomyocytes using an MTT assay, and the viability rates were 73.2 ± 6.5, 54.1 ± 4.3 and 105.4 ± 8.0% in the LT, LH and LL groups, respectively. These data demonstrated that low-dose ALA treatment increased the survival of cardiomyocytes and protected the function of the cardiovascular system.

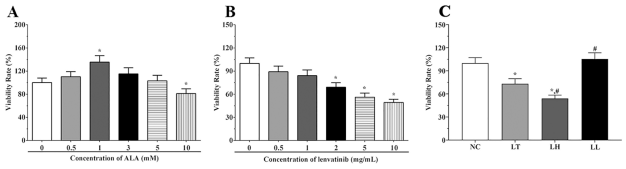

Fig. 1. Effect of 5-ALA and lenvatinib on cardiomyocytes. (A) Effect of 5-ALA on cardiomyocytes. (B) Effect of lenvatinib on cardiomyocytes. (C) Viability rate of cardiomyocytes. $^{*}p < 0.05$ vs. NC group. $^{\#}p < 0.05$ vs. LT group.

Activation of the PI3K/AKT/mTOR Signaling Pathway in Cells and Tissues

Fig. 2 shows that the ratios of p-AKT/AKT in each group of cardiomyocytes were 1.18 ± 0.09, 0.92 ± 0.07, 0.52 ± 0.04 and 1.23 ± 0.09. The ratios of p-mTOR/mTOR in each group of cardiomyocytes were 0.96 ± 0.07, 0.84 ± 0.06, 0.62 ± 0.05 and 1.10 ± 0.08. The ratios of p-ERK/ERK in each group of cardiomyocytes were 0.39 ± 0.03, 0.43 ± 0.04, 0.10 ± 0.01 and 0.37 ± 0.03. The expression levels of Nrf2 in each group of cardiomyocytes were 0.73 ± 0.06, 0.59 ± 0.05, 0.38 ± 0.03 and 1.10 ± 0.08. The expression levels of HO-1 in each group of cardiomyocytes were 0.97 ± 0.07, 0.92 ± 0.07, 0.55 ± 0.04 and 1.46 ± 0.11. The expression levels of HIF-1α in each group of cardiomyocytes were 0.39 ± 0.03, 1.06 ± 0.08, 1.28 ± 0.10 and 0.65 ± 0.05. Fig. 3 shows that the ratios of p-AKT/AKT in each group of tissue samples were 0.82 ± 0.06, 0.92 ± 0.07, 0.62 ± 0.05 and 1.14 ± 0.09. The ratios of p-mTOR/mTOR in each group of tissue samples were 1.24 ± 0.10, 1.13 ± 0.09, 0.53 ± 0.04 and 1.28 ± 0.10. The ratios of p-ERK/ERK in each group of tissue samples were 0.57 ± 0.05, 0.33 ± 0.03, 0.15 ± 0.01 and 0.65 ± 0.05. The expression levels of Nrf2 in each group of tissue samples were 1.45 ± 0.11, 1.18 ± 0.09, 0.85 ± 0.07 and 1.33 ± 0.10. The expression levels of HO-1 in each group of tissue samples were 1.57 ± 0.12, 1.37 ± 0.11, 1.04 ± 0.08 and 1.37 ± 0.11. The expression levels of HIF-1α in each group of tissue samples were 0.56 ± 0.04, 1.49 ± 0.11, 1.57 ± 0.12 and 0.70 ± 0.05. These results indicated that the PI3K/AKT/mTOR/ERK signaling pathway was inhibited after lenvatinib treatment, leading to the downregulation of Nrf2 and HO-1, which are downstream molecules of the PI3K/AKT signaling pathway. The downregulation of these molecules induced the upregulation of HIF-1α, reflecting the oxidative stress status in cardiomyocytes. However, low dose ALA treatment reduced these effects, thereby showing a protective role, while high dose ALA treatment enhanced these effects.

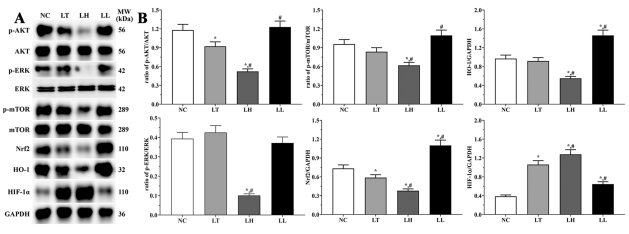

Fig. 2. Expression of PI3K/AKT/mTOR signaling pathway in each group of cardiomyocytes. (A) Expression of p-AKT, AKT, p-mTOR, mTOR, p-ERK, ERK, Nrf2, HO-1, and HIF-1α. (B) Quantitative analysis of each protein. *$p < 0.05$ vs. NC group. #$p < 0.05$ vs. LT group.

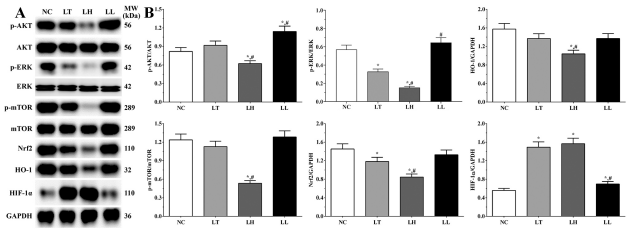

Fig. 3. Expression of PI3K/AKT/mTOR signaling pathway in tissue samples. (A) Expression of p-AKT, AKT, p-mTOR, mTOR, p-ERK, ERK, Nrf2, HO-1, and HIF-1α. (B) Quantitative analysis of each protein. *$p < 0.05$ vs. NC group. #$p < 0.05$ vs. LT group.

Expression of Cardioprotective Proteins in Cells and Tissues

Fig. 4 shows that the ratios of p-NF-κB/NF-κB in each group of cardiomyocytes were 0.81 ± 0.06, 0.64 ± 0.05, 0.20 ± 0.02 and 0.54 ± 0.04. The expression of ICAM-1 in each group of cardiomyocytes was 1.10 ± 0.08, 1.37 ± 0.11, 1.61 ± 0.12 and 1.11 ± 0.09. The expression levels of VCAM in each group of cardiomyocytes were 0.88 ± 0.07, 1.50 ± 0.12, 1.93 ± 0.15 and 0.95 ± 0.07. The expression levels of ANG I (angiotensin I) in each group of cardiomyocytes were 0.55 ± 0.04, 1.00 ± 0.08, 1.41 ± 0.11 and 0.88 ± 0.07. The expression levels of ANG II in each group of cardiomyocytes were 0.86 ± 0.07, 1.24 ± 0.10, 1.45 ± 0.11 and 0.83 ± 0.06. The expression levels of eNOS in each group of cardiomyocytes were 0.98 ± 0.08, 0.80 ± 0.06, 0.45 ± 0.03 and 1.00 ± 0.08. Fig. 5 shows that the ratios of p-NF-κB/NF-κB in each group of tissue samples were 1.49 ± 0.11, 0.72 ± 0.06, 0.38 ± 0.03 and 1.17 ± 0.09. The expression levels of ICAM-1 in each group of tissue samples were 0.95 ± 0.07, 1.24 ± 0.10, 1.12 ± 0.09 and 0.88 ± 0.07. The expression levels of VCAM in each group of tissue samples were 0.76 ± 0.06, 1.15 ± 0.09, 1.18 ± 0.09 and 0.76 ± 0.06. The expression levels of ANG I in each group of tissue samples were 0.84 ± 0.06, 1.43 ± 0.11, 1.40 ± 0.11 and 0.94 ± 0.07. The expression levels of ANG II in each group of tissue samples were 1.34 ± 0.10, 1.64 ± 0.13, 1.77 ± 0.14 and 0.78 ± 0.06. The expression levels of eNOS in each group of tissue samples were 1.08 ± 0.08, 0.37 ± 0.03, 0.05 ± 0.01 and 0.70 ± 0.05. These results showed that lenvatinib treatment increased the expression of ICAM-1 and VCAM, leading to the adhesion of inflammatory cells to the vessel wall. Moreover, lenvatinib treatment also increased ANG expression while decreasing eNOS expression, thereby inducing vasoconstriction. However, high-dose ALA promoted these effects, while low dose ALA reduced these effects, indicating that low-dose ALA may have a protective role.

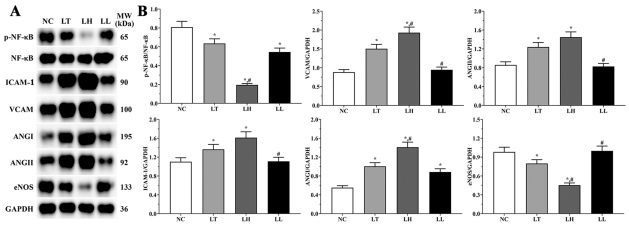

Fig. 4. Expression of cardiovascular disease-inducible factors in each endothelial cell group. (A) Expression of p-NF-κB, NF-κB, ICAM-1, VCAM, ANG I, ANG II, and eNOS. (B) Quantitative analysis of each protein. *$p < 0.05$ vs. NC group. #$p < 0.05$ vs. LT group.

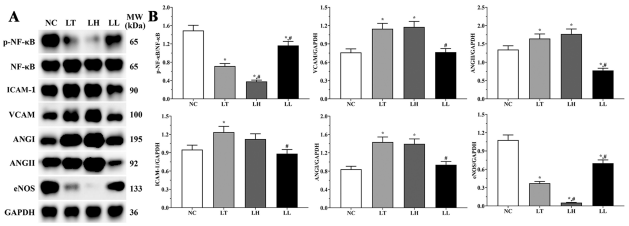

Fig. 5. Expression of cardiovascular disease-inducible factors in mouse aorta tissue in each group. (A) Expression of p-NF-κB, NF-κB, ICAM-1, VCAM, ANG I, ANG II, and eNOS. (B) Quantitative analysis of each protein. *$p < 0.05$ vs. NC group. #$p < 0.05$ vs. LT group.

Expression of NF-κB Downstream Genes in Cells and Tissues

Fig. 6 shows that the expression levels of *Nrf2* mRNA in each group of cardiomyocytes were 0.85 ± 0.07, 0.71 ± 0.05, 0.53 ± 0.05 and 1.12 ± 0.10. The expression levels of *HO-1* mRNA in each group of cardiomyocytes were 0.96 ± 0.09, 0.83 ± 0.08, 0.64 ± 0.05 and 1.23 ± 0.12. The expression levels of *Fas* mRNA in each group of cardiomyocytes were 0.81 ± 0.06, 0.98 ± 0.08, 1.15 ± 0.09 and 0.64 ± 0.07. The expression levels of *CDK6* (cyclin dependent kinase 6) mRNA in each group of cardiomyocytes were 0.71 ± 0.06, 0.62 ± 0.04, 0.48 ± 0.04 and 0.93 ± 0.10.

Fig. 7 shows that the expression levels of *Nrf2* mRNA in each group of tissue samples were 1.23 ± 0.10, 1.08 ± 0.09, 0.82 ± 0.07 and 1.51 ± 0.14. The expression levels of *HO-1* mRNA in each group of tissue samples were 1.02 ± 0.11, 0.91 ± 0.09, 0.76 ± 0.08 and 1.33 ± 0.14. The expression levels of *Fas* mRNA in each group of tissue samples were 0.83 ± 0.7, 0.98 ± 0.10, 1.31 ± 0.13 and 0.66 ± 0.06. The expression levels of *CDK6* in each group of tissue samples were 0.92 ± 0.09, 0.80 ± 0.07, 0.61 ± 0.05 and 1.36 ± 0.15. These results showed that the lenvatinib treatment reduced the expression of NF-κB downstream genes, and high dose of ALA enhanced these effects, while a low dose of ALA treatment reduced these effects, indicating that ALA regulates the expression of NF-κB downstream genes in a dose dependent manner.

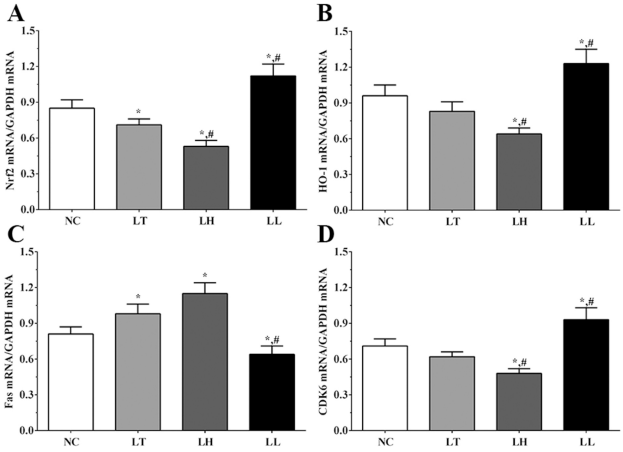

Fig. 6. Expression of Nrf2, HO-1, Fas and CDK6 in each endothelial cell group. (A) Expression of *Nrf2* mRNA. (B) Expression of *HO-1* mRNA. (C) Expression of *Fas* mRNA. (D) Expression of *CDK6* mRNA. *$p < 0.05$ vs. NC group. #$p < 0.05$ vs. LT group.

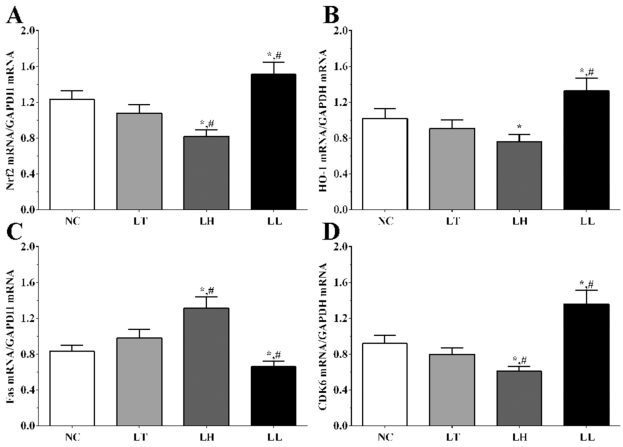

Fig. 7. Expression of *Nrf2*, *HO-1*, *Fas* and *CDK6* genes in mouse aorta tissue. (A) Expression of *Nrf2* mRNA. (B) Expression of *HO-1* mRNA. (C) Expression of *Fas* mRNA. (D) Expression of *CDK6* mRNA. *$p < 0.05$ vs. NC group. #$p < 0.05$ vs. LT group.

Concentration of Key Cardiovascular Protective Cytokines in Cultured Media and Serum Samples

Fig. 8 shows that the concentrations of NO in the cultured media of cardiomyocytes in the NC, LT, LH and LL groups were 142.3 ± 13.2, 120.1 ± 10.0, 99.6 ± 8.1 and 156.4 ± 15.4 μmol/L, respectively. Lenvatinib decreased the concentration of NO in the media of cardiomyocytes and further reduced it under high-dose ALA treatment. The concentration of NO increased under low-dose ALA treatment. The concentrations of ANG in the NC, LT, LH and LL groups were 184.2 ± 16.3, 216.4 ± 19.1, 245.9 ± 21.5 and 162.3 ± 13.0 pg/mL, respectively. The concentration of ANG increased under high-dose ALA treatment but de-

creased to nearly normal levels under low-dose ALA treatment. The ratios of ROS in the LT, LH and LL groups compared to the NC group were 1.13 ± 0.08, 1.37 ± 0.10 and 0.81 ± 0.06, respectively. High-dose ALA treatment increased the concentration of ROS compared to the NC and LT groups, but low-dose ALA treatment decreased the concentration of ROS. The concentrations of VEGF-α in the NC, LT, LH and LL groups were 56.2 ± 2.5, 48.2 ± 2.0, 44.6 ± 1.8 and 61.4 ± 2.6 pg/mL, respectively. Lenvatinib treatment significantly decreased the concentration of VEGF-α, and high-dose ALA treatment increased this effect. However, low-dose ALA treatment increased the concentration of VEGF-α.

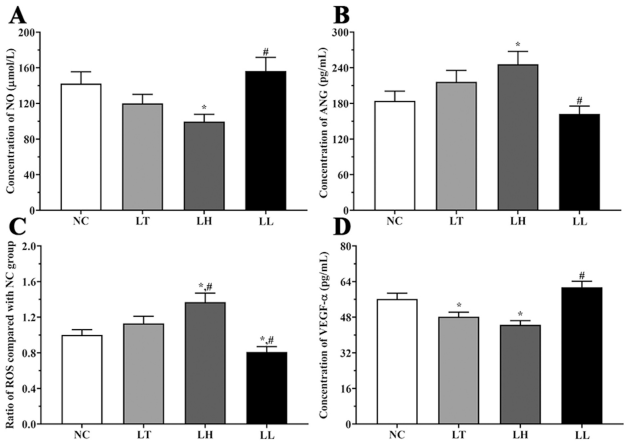

Fig. 8. Concentration of NO, ANG, ROS and VEGF-α in each group of endothelial cell cultured medium. (A) Concentration of NO. (B) Concentration of ANG. (C) Concentration of ROS. (D) Concentration of VEGF-α. *$p < 0.05$ vs. NC group. #$p < 0.05$ vs. LT group.

Fig. 9 shows that the concentrations of NO in serum samples of mice in the NC, LT, LH and LL groups were 202.2 ± 11.3, 185.2 ± 10.1, 162.3 ± 10.6 and 228.5 ± 13.2 μmol/L, respectively. The concentrations of ANG in serum samples of mice in the NC, LT, LH and LL groups were 176.2 ± 16.8, 198.1 ± 18.2, 231.4 ± 21.0 and 152.2 ± 12.7 pg/mL, respectively. The ratios of ROS in the LT, LH and LL groups compared to the NC group were 1.33 ± 0.12, 1.78 ± 0.18 and 0.72 ± 0.04, respectively. The ratio of ROS was significantly increased after lenvatinib treatment and further increased after high dose ALA treatment, but low dose ALA treatment reversed this trend. The concentrations of VEGF-α in serum samples of mice in the NC, LT, LH and LL groups were 66.2 ± 2.8, 62.5 ± 2.3, 58.4 ± 1.9 and 72.0 ± 3.0 pg/mL, respectively. The concentration of VEGF-α was significantly decreased under lenvatinib treatment in combination with high-dose ALA treatment but increased under lenvatinib treatment in combination with low-dose ALA treatment. These results showed that low-dose ALA treatment increased the secretion of cardioprotective factors but that high-dose ALA treatment decreased this effect, indicating that low-dose ALA treatment may have a protective role in cardiomyocytes after lenvatinib treatment.

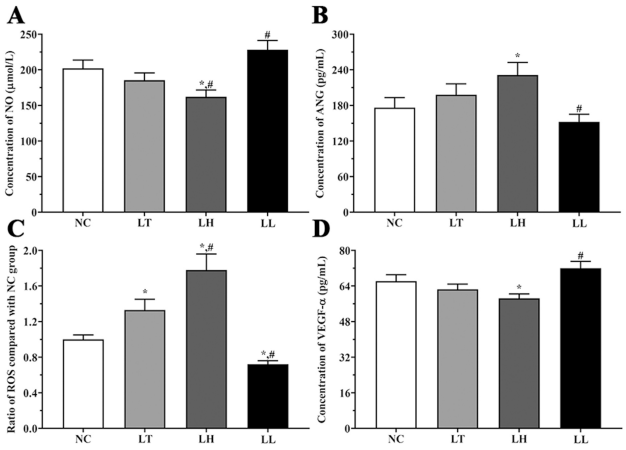

Fig. 9. Concentration of NO, ANG, ROS and VEGF-α in each mouse serum sample group. (A) Concentration of NO. (B) Concentration of ANG. (C) Concentration of ROS. (D) Concentration of VEGF-α. *$p < 0.05$ vs. NC group. #$p < 0.05$ vs. LT group.

Discussion

Previous studies have shown that lenvatinib decreases the angiogenesis in a xenograft model and exhibits antitumor activity [5,17,18]. 5-Aminolevulinic acid hydrochloride is a natural compound acquired from various foods that activates mitochondrial respiratory function and the production of ATP (Adenosine triphosphate) for heme production [19]. ALA treatment may exert a protective role in cardiomyocytes under lenvatinib stimulation. In addition, ALA also promoted the function of cisplatin-based chemotherapy in the treatment of lung cancer [20], and ALA also reduced the production of proinflammation cytokines, which benefits IBD (Inflammation Bowel Disease) treatment [21]. A recent study also showed that ALA reduced the doxorubicin-induced ferroptosis and cardiotoxicity in cardiomyocytes [22]. Hence, we thought ALA might be an effective drug in cardiovascular disease treatment. The PI3K/AKT signaling pathway is an important pathway in the regulation of cellular proliferation and angiogenesis [23]. Growth factors, such as VEGF-α, activate PI3K via direct or indirect recruitment. PI3K activates phosphatidylinositol-3,4,5-triphosphate (PIP3) and recruits AKT to the plasma membrane, which further induces the activation of downstream molecules, including mTOR, via phosphorylation [24]. Phosphorylated AKT is critical for the regulation of cellular proliferation via the inhibition of the apoptosis process and phosphorylation to induce interaction with various apoptotic members [25,26]. A previous

study has reported that inhibition of the PI3K/AKT signaling pathway increased the cellular apoptosis rate [27]. Another study has also reported that activation of PI3K or AKT protected cells from anoikis but that inhibition of PI3K or AKT induces anoikis [28]. According to a published paper, ALA inhibited the expression of the PI3K/AKT/mTOR pathway, thereby reducing the proliferation of cancer cells [29].

Activation of the ERK signaling pathway promotes the dissociation of Nrf2 from the Nrf2/KEAP1 (Kelch-like ECH-associated protein-1) polymer, which leads to the activation and translocation of Nrf2 into the nucleus. Nuclear Nrf2 forms Nrf2/MafG (MAF BZIP Transcription Factor G) by binding with MafG. The Nef2/MafG complex further binds with ARE (antioxidant response element) and activates the transcription and expression of downstream molecules, such as HO-1, to exert an antioxidative effect [30,31]. ALA induced the activation of the Nrf2/HO-1 pathway, thereby increasing the expression of HO-1, which protects cardiomyocytes from H_2O_2 induced by cardiac hypertrophy [32]. NF-κB was first found in 1986 as a critical transcription factor for the expression of the k-chain of immunoglobulins in B-cell [33]. Induction of HO-1 expression is a critical step of the phase II antioxidative defense mechanism, in which NF-κB and Nrf2 also participate as transcription factors [34]. Nrf2 is a transcription factor containing six Nrf-2-ECH homolog (Neh) domains, and it performs multiple molecular functions. A recent study showed that activation of Nrf2 and downstream molecules alleviated cellular injury via suppression of oxidative stress [35]. Another study showed that activation of Nrf2 increased the expression of HO-1, which further increased the antioxidative ability of cells. However, inhibition of the activation of the PI3K and MAPK (Mitogen-Activated Protein Kinase) signaling pathways resulted in downregulation of Nrf2 and HO-1 [36]. In this experiment, we showed that the PI3K/AKT/mTOR/ERK signaling pathway was inhibited after treatment with lenvatinib. Lenvatinib further decreased the expression of Nrf2 and HO-1, which damaged the antioxidative system of cardiomyocytes, leading to the accumulation of reactive oxygen species and the upregulation of HIF-1α. Moreover, low-dose ALA treatment reduced this effect, but high-dose ALA treatment enhanced this effect, showing that low-dose ALA treatment has a protective role in cardiomyocytes.

HIF-1α is a member of the hypoxia-inducible factor (HIF) family and is an indicator of oxidative stress. HIF-1α is constitutively expressed in cells. HIF-1α is degraded in proteasomes, and it remains stable under hypoxia [37]. HIF-1α also regulates the expression of vascular endothelial growth factor-α (VEGF-α), SERCA2 and ABCG2 in cardiomyocytes, vascular cardiomyocytes and vascular smooth muscle cells [38]. eNOS is a nitric oxide synthase (NOS) subtype, and it is primarily regulated by the phosphatidylinositol 3-kinase (PI3K)/serine threonine protein kinase B (AKT) pathway [39]. Angiotensinogen was first discovered in 1898, and angiotensin-converting enzyme (ACE) is a key component of the renin-angiotensin system (RAS) [40]. Angiotensin is produced in the liver from angiotensinogen and released into circulating blood where it is converted into angiotensin I (ANG (Angiopoietin) I) and ANGII. ANG I and II play important roles in the proliferation of vascular smooth muscle cells and the pathogenesis of cerebrovascular remodeling, which contributes to the development of cardiovascular disease [41]. eNOS binds with nicotinamide adenine dinucleotide phosphate (NADPH), flavin mononucleotide (FMN) and flavin adenine dinucleotide (FAD) via C-terminal bonds and with tetrahydrobiopterin4 (BH4) and O_2 in the heme-binding region [42]. Under physiological conditions, cardiomyocytes primarily produce NO via eNOS, which acts as a multifunctional signaling molecule that reduces the production of reactive oxygen species (ROS) and lipid peroxidation [43]. NO also inhibits platelet adhesion, platelet aggregation, inflammatory cell infiltration and smooth muscle cell (SMC) proliferation, which is the initial step of cardiovascular disease [44]. A previous study showed that activation of eNOS and reduction of ROS produce a protective effect in cardiovascular disease via inhibition of the release of cell adhesion molecule (ICAM-1) and vascular cell adhesion molecule (VCAM-1) from cardiomyocytes, which play a protective role [45]. Lenvatinib treatment increased the expression of HIF-1α, leading to upregulation of ANGs and downregulation of eNOS, which further increased the concentration of ROS. Upregulation of ICAM-1 and VCAM then follows, thus enhancing the ability of inflammatory cells to adhere to blood vessels, which is the critical step in development of cardiovascular disease. Low-dose ALA treatment reversed this trend, suggesting that low-dose ALA treatment may have a protective role in cardiomyocytes.

Conclusions

Low-dose 5-ALA treatment alleviated lenvatinib-induced damage in cardiomyocytes via activation of antioxidative stress-related enzymes and reduction in the release of cardiovascular disease-inducible factors, thereby reducing the side effects of lenvatinib treatment.

Availability of Data and Materials

Data of this manuscript is available from the corresponding author based on reasonable request.

Author Contributions

YS and FH performed the most of the experiments and wrote the manuscript. HF contributes to the data analysis and mice model construction. SL contributes to the sample collection. CL and CH designed the experiments and revised the manuscript. All authors contributed to editorial

changes in the manuscript. All authors read and approved the final manuscript. All authors have participated sufficiently in the work and agreed to be accountable for all aspects of the work.

Ethics Approval and Consent to Participate

This study was approved by the Institution's Ethics Committee for Investigation of Tianjin Medical University (SYXK2021-007), and all 20 animals received humane care in compliance with the Public Health Service Policy on Humane Care and Use of Laboratory Animals.

Acknowledgment

Not applicable.

Funding

The research is supported by National Natural Science Foundation of China (No. 81970303), Tianjin Key Medical Discipline (Specialty) Construction Project (No. TJYXZDXK-054B), Medical science research project of Hebei Province (No. 20221849), Science and technology project of Tianjin Health Commission (No. TJWJ2022MS022), 2021 Excellent Young Talents Training Fund of Tianjin Fourth Central Hospital (No. TJDSZXYY20210018), The Natural Science Foundation of Tianjin (No. 21JCYBJC00250), Military special research project (No. 21JSZ23).

Conflict of Interest

The authors declare no conflict of interest.

References

[1] Golabi P, Fazel S, Otgonsuren M, Sayiner M, Locklear CT, Younossi ZM. Mortality assessment of patients with hepatocellular carcinoma according to underlying disease and treatment modalities. Medicine. 2017; 96: e5904.

[2] Al-Salama ZT, Syed YY, Scott LJ. Lenvatinib: A Review in Hepatocellular Carcinoma. Drugs. 2019; 79: 665–674.

[3] Motzer RJ, Hutson TE, Glen H, Michaelson MD, Molina A, Eisen T, *et al*. Lenvatinib, everolimus, and the combination in patients with metastatic renal cell carcinoma: a randomised, phase 2, open-label, multicentre trial. The Lancet. Oncology. 2015; 16: 1473–1482.

[4] Patel UJ, May M. Lenvatinib in the Treatment of Differentiated Thyroid Cancer and Advanced Renal Cell Carcinoma. Journal of the Advanced Practitioner in Oncology. 2017; 8: 757–764.

[5] Sueta D, Suyama K, Sueta A, Tabata N, Yamashita T, Tomiguchi M, *et al*. Lenvatinib, an oral multi-kinases inhibitor, -associated hypertension: Potential role of vascular endothelial dysfunction. Atherosclerosis. 2017; 260: 116–120.

[6] Gunaydin Akyildiz A, Boran T, Jannuzzi AT, Alpertunga B. Mitochondrial dynamics imbalance and mitochondrial dysfunction contribute to the molecular cardiotoxic effects of lenvatinib. Toxicology and Applied Pharmacology. 2021; 423: 115577.

[7] 7. Gao XL, Zhang J, Dai ZH, Luo D, He RF, Li ML. Anti-tumor drug lenvatinib induced cardiotoxicity via mitochondrial oxidative stress and apoptosis. Journal of Molecular and Cellular Cardiology. 2020;140:25.

[8] Owari T, Tanaka N, Nakai Y, Miyake M, Anai S, Kishi S, *et al*. 5-Aminolevulinic acid overcomes hypoxia-induced radiation resistance by enhancing mitochondrial reactive oxygen species production in prostate cancer cells. British Journal of Cancer. 2022; 127: 350–363.

[9] Eatz TA, Eichberg DG, Lu VM, Di L, Komotar RJ, Ivan ME. Intraoperative 5-ALA fluorescence-guided resection of high-grade glioma leads to greater extent of resection with better outcomes: a systematic review. Journal of Neuro-oncology. 2022; 156: 233–256.

[10] Yang W, Xu H, Liu Q, Liu C, Hu J, Liu P, *et al*. 5-Aminolevulinic acid hydrochloride loaded microbubbles-mediated sonodynamic therapy in pancreatic cancer cells. Artificial Cells, Nanomedicine, and Biotechnology. 2020; 48: 1178–1188.

[11] Inoue K. 5-Aminolevulinic acid-mediated photodynamic therapy for bladder cancer. International Journal of Urology. 2017; 24: 97–101.

[12] Fujino M, Nishio Y, Ito H, Tanaka T, Li XK. 5-Aminolevulinic acid regulates the inflammatory response and alloimmune reaction. International Immunopharmacology. 2016; 37: 71–78.

[13] Steinbach P, Kriegmair M, Baumgartner R, Hofstädter F, Knüchel R. Intravesical instillation of 5-aminolevulinic acid: the fluorescent metabolite is limited to urothelial cells. Urology. 1994; 44: 676–681.

[14] Wang R, Yamada T, Arai S, Fukuda K, Taniguchi H, Tanimoto A, *et al*. Distribution and Activity of Lenvatinib in Brain Tumor Models of Human Anaplastic Thyroid Cancer Cells in Severe Combined Immune Deficient Mice. Molecular Cancer Therapeutics. 2019; 18: 947–956.

[15] Saitoh S, Okano S, Nohara H, Nakano H, Shirasawa N, Naito A, *et al*. 5-aminolevulinic acid (ALA) deficiency causes impaired glucose tolerance and insulin resistance coincident with an attenuation of mitochondrial function in aged mice. PloS one. 2018; 13: e0189593.

[16] Livak KJ, Schmittgen TD. Analysis of relative gene expression data using real-time quantitative PCR and the 2(-Delta Delta C(T)) Method. Methods (San Diego, Calif.). 2001; 25: 402–408.

[17] Koyama N, Saito K, Nishioka Y, Yusa W, Yamamoto N, Yamada Y, *et al*. Pharmacodynamic change in plasma angiogenic proteins: a dose-escalation phase 1 study of the multi-kinase inhibitor lenvatinib. BMC Cancer. 2014; 14: 530.

[18] Ikuta K, Yano S, Trung VT, Hanibuchi M, Goto H, Li Q, *et al*. E7080, a multi-tyrosine kinase inhibitor, suppresses the progression of malignant pleural mesothelioma with different proangiogenic cytokine production profiles. Clinical Cancer Research. 2009; 15: 7229–7237.

[19] Ishikawa T, Takahashi K, Ikeda N, Kajimoto Y, Hagiya Y, Ogura SI, *et al*. Transporter-Mediated Drug Interaction Strategy for 5-Aminolevulinic Acid (ALA)-Based Photodynamic Diagnosis of Malignant Brain Tumor: Molecular Design of ABCG2 Inhibitors. Pharmaceutics. 2011; 3: 615–635.

[20] Kawamura K, Matsushima H, Sakai H, Iwashima A, Nakamura S, Kojima T, *et al*. A Randomized Phase 2 Study of 5-Aminolevulinic Acid Hydrochloride and Sodium Ferrous Citrate for the Prevention of Nephrotoxicity Induced by Cisplatin-Based Chemotherapy of Lung Cancer. Oncology. 2022; 100: 620–632.

[21] Yadav V, Mai Y, McCoubrey LE, Wada Y, Tomioka M, Kawata S, *et al*. 5-Aminolevulinic Acid as a Novel Therapeutic for Inflammatory Bowel Disease. Biomedicines. 2021; 9: 578.

[22] Abe K, Ikeda M, Ide T, Tadokoro T, Miyamoto HD, Furusawa S, *et al*. Doxorubicin causes ferroptosis and cardiotoxicity by intercalating into mitochondrial DNA and disrupting Alas1-dependent heme synthesis. Science Signaling. 2022; 15: eabn8017.

[23] Zhang Y, Lin X, Dai Y, Hu X, Zhu H, Jiang Y, *et al*. Endometrial stem cells repair injured endometrium and induce angiogenesis via AKT and ERK pathways. Reproduction (Cambridge, England). 2016; 152: 389–402.

[24] Bianco C, Strizzi L, Rehman A, Normanno N, Wechselberger C, Sun Y, *et al*. A Nodal- and ALK4-independent signaling pathway activated by Cripto-1 through Glypican-1 and c-Src. Cancer Research. 2003; 63: 1192–1197.

[25] Liu Y, Xing H, Weng D, Song X, Qin X, Xia X, *et al*. Inhibition of Akt signaling by SN-38 induces apoptosis in cervical cancer. Cancer Letters. 2009; 274: 47–53.

[26] Sibal L, Aldibbiat A, Agarwal SC, Mitchell G, Oates C, Razvi S, *et al*. Circulating endothelial progenitor cells, endothelial function, carotid intima-media thickness and circulating markers of endothelial dysfunction in people with type 1 diabetes without macrovascular disease or microalbuminuria. Diabetologia. 2009; 52: 1464–1473.

[27] Ceradini DJ, Yao D, Grogan RH, Callaghan MJ, Edelstein D, Brownlee M, *et al*. Decreasing intracellular superoxide corrects defective ischemia-induced new vessel formation in diabetic mice. The Journal of Biological Chemistry. 2008; 283: 10930–10938.

[28] Eustace AJ, Conlon NT, McDermott MSJ, Browne BC, O'Leary P, Holmes FA, *et al*. Development of acquired resistance to lapatinib may sensitise HER2-positive breast cancer cells to apoptosis induction by obatoclax and TRAIL. BMC Cancer. 2018; 18: 965.

[29] Xie J, Wang S, Li Z, Ao C, Wang J, Wang L, *et al*. 5-aminolevulinic acid photodynamic therapy reduces HPV viral load via autophagy and apoptosis by modulating Ras/Raf/MEK/ERK and PI3K/AKT pathways in HeLa cells. Journal of Photochemistry and Photobiology. B, Biology. 2019; 194: 46–55.

[30] Digicaylioglu M, Lipton SA. Erythropoietin-mediated neuroprotection involves cross-talk between Jak2 and NF-kappaB signalling cascades. Nature. 2001; 412: 641–647.

[31] Katsuoka F, Motohashi H, Engel JD, Yamamoto M. Nrf2 transcriptionally activates the mafG gene through an antioxidant response element. The Journal of Biological Chemistry. 2005; 280: 4483–4490.

[32] Zhao M, Guo H, Chen J, Fujino M, Ito H, Takahashi K, *et al*. 5-aminolevulinic acid combined with sodium ferrous citrate ameliorates H2O2-induced cardiomyocyte hypertrophy via activation of the MAPK/Nrf2/HO-1 pathway. American Journal of Physiology. Cell Physiology. 2015; 308: C665–C672.

[33] Sen R, Baltimore D. Multiple nuclear factors interact with the immunoglobulin enhancer sequences. Cell. 1986; 46: 705–716.

[34] Rubiolo JA, Vega FV. Resveratrol protects primary rat hepatocytes against necrosis induced by reactive oxygen species. Biomedicine & Pharmacotherapy. 2008; 62: 606–612.

[35] Herrera-Arozamena C, Martí-Marí O, Estrada M, de la Fuente Revenga M, Rodríguez-Franco MI. Recent Advances in Neurogenic Small Molecules as Innovative Treatments for Neurodegenerative Diseases. Molecules (Basel, Switzerland). 2016; 21: 1165.

[36] Genc K, Egrilmez MY, Genc S. Erythropoietin induces nuclear translocation of Nrf2 and heme oxygenase-1 expression in SH-SY5Y cells. Cell Biochemistry and Function. 2010; 28: 197–201.

[37] Wong BW, Kuchnio A, Bruning U, Carmeliet P. Emerging novel functions of the oxygen-sensing prolyl hydroxylase domain enzymes. Trends in Biochemical Sciences. 2013; 38: 3–11.

[38] Nagy BM, Nagaraj C, Egemnazarov B, Kwapiszewska G, Stauber RE, Avian A, *et al*. Lack of ABCG2 Leads to Biventricular Dysfunction and Remodeling in Response to Hypoxia. Frontiers in Physiology. 2017; 8: 98.

[39] Gong X, Shao L, Fu YM, Zou Y. Effects of olmesartan on endothelial progenitor cell mobilization and function in carotid atherosclerosis. Medical Science Monitor: International Medical Journal of Experimental and Clinical Research. 2015; 21: 1189–1193.

[40] Rodriguez R, Fernandez EM. Role of angiotensin II in treatment of refractory distributive shock. American Journal of Health-system Pharmacy: AJHP: Official Journal of the American Society of Health-System Pharmacists. 2019; 76: 101–107.

[41] Myburgh JA, Higgins A, Jovanovska A, Lipman J, Ramakrishnan N, Santamaria J, *et al*. A comparison of epinephrine and norepinephrine in critically ill patients. Intensive Care Medicine. 2008; 34: 2226–2234.

[42] Solini A, Rossi C, Duranti E, Taddei S, Natali A, Virdis A. Saxagliptin prevents vascular remodeling and oxidative stress in db/db mice. Role of endothelial nitric oxide synthase uncoupling and cyclooxygenase. Vascular Pharmacology. 2016; 76: 62–71.

[43] Sukhovershin RA, Ghebremariam YT, Cooke JP. Lansoprazole worsens asthma control in poor metabolizers: is nitric oxide involved? Annals of the American Thoracic Society. 2015; 12: 1109–1110.

[44] Sharma DK, Manral A, Saini V, Singh A, Srinivasan BP, Tiwari M. Novel diallyldisulfide analogs ameliorate cardiovascular remodeling in rats with L-NAME-induced hypertension. European Journal of Pharmacology. 2012; 691: 198–208.

[45] Su Y, Qadri SM, Wu L, Liu L. Methylglyoxal modulates endothelial nitric oxide synthase-associated functions in EA.hy926 endothelial cells. Cardiovascular Diabetology. 2013; 12: 134.